Resolving vibrational wave-packet dynamics of D_2^+ using multicolor probe pulses

Yusuke Furukawa,[1] Yasuo Nabekawa,[1,*] Tomoya Okino,[1,2] A. Amani Eilanlou,[1] Eiji J. Takahashi,[1] Pengfei Lan,[1] Kenichi L. Ishikawa,[3] Takeshi Sato,[3] Kaoru Yamanouchi,[1,2] and Katsumi Midorikawa[1]

[1] *Laser Technology Laboratory, RIKEN ASI, 2-1 Hirosawa, Wako-shi, Saitama 351-0198, Japan*

[2] *Department of Chemistry, School of Science, the University of Tokyo, 7-3-1 Hongo, Bunkyo, Tokyo 113-0033, Japan*

[3] *Photon Science Center, Graduate School of Engineering, the University of Tokyo,*
7-3-1 Hongo, Bunkyo-ku, Tokyo 113-8656, Japan
**Corresponding author: nabekawa@riken.jp*

Received April 16, 2012; accepted May 18, 2012;
posted May 22, 2012 (Doc. ID 166818); published July 12, 2012

We demonstrate the generation and real-time observation of the vibrational wave packet of D_2^+ by using a sub-10-fs extreme UV high-harmonic pump pulse and a three-color probe laser pulse whose wavelength ranges from near-IR to vacuum UV. This multicolor pump–probe scheme can provide us with a powerful experimental tool for investigating a variety of wave packets evolving with a time scale of ~20 fs. © 2012 Optical Society of America

OCIS codes: 320.7120, 020.4180, 340.7480, 190.7110.

The vibrational motion of a diatomic molecule [1] is one of the prominent physical systems that can reveal the fundamental nature of the quantum dynamics of matter [2]. The generation, observation, and control of a vibrational wave packet are the key issues in utilizing the quantum nature of this system for applications. The simpler the system, the closer we can approach the essence of the system. Therefore, a singly charged hydrogen or deuterium molecule (H_2^+ or D_2^+), which is the simplest molecule containing only one electron, has strongly attracted our interest.

The most significant issue in the real-time measurement of the vibrational wave-packet dynamics of D_2^+ (or H_2^+) (see [3], and references therein) is the time resolution. The durations of both pump and probe pulses should be much shorter than the vibrational period, typically less than 10 fs. The hollow-core fiber compression technique combined with a near-IR (NIR) Ti:sapphire laser is now the most feasible method for obtaining such a short pulse duration, and hence, an NIR Ti:sapphire laser pulse has been used as a probe in most related studies, except for those reported in [4].

In the present work, we have exhibited a novel pump–probe scheme utilizing harmonic fields of a sub-15-fs Ti:sapphire laser pulse [5]. A wave packet of D_2^+ has been generated via the one-photon ionization of D_2 by irradiating a sub-10-fs extreme ultraviolet (XUV) pulse with a photon energy of ~17.1 eV. Then we applied a probe pulse containing a three-color harmonic field after some delay. We find that partial wave-packet (PWP) components contained in the generated wave packet at the lowest few vibrational energy levels ($\nu = 0$–4) and the middle range levels ($\nu = 3$–7 and $\nu = 9$–13) are resolved by the fifth harmonic, third harmonic, and fundamental fields in the probe pulse, the photon energies of which are ~7.6 eV, ~4.7 eV, and ~1.55 eV, respectively. This is the first observation, to the best of our knowledge, of molecular motion with a period less than 25 fs by utilizing multiple harmonic fields ranging from NIR to XUV.

The experimental setup is similar to that adopted in the nonlinear and linear autocorrelation measurement of an attosecond pulse train [6–10] except for the specifications of the laser system. The chirped pulse amplification (CPA) system of a Ti:sapphire laser [5] delivers driving laser pulses with a pulse duration of 14 fs to generate harmonic fields ranging from the 3rd to 19th order (deep UV to XUV) region. The repetition rate of the driving laser pulse was 100 Hz. The generated harmonic fields are reflected efficiently with a pair of Si harmonic separator mirrors, while the fundamental laser pulse is strongly attenuated. The Si mirror pair also splits the incident fundamental and harmonic fields spatially into two replicas, one of which acts as an XUV pump pulse with temporal advancement and the other of which acts a three-color probe pulse with delay, by translating one of the Si mirrors with a piezo actuator. We will explain later the reason why the identical replica pulses can be discriminated with the time order, although we do not separate explicitly the pump and probe pulses with the wavelengths [11–13]. All the reflected pulses from the Si mirror pair are introduced into a vacuum chamber containing a velocity map ion (VMI) spectrometer after passing through an aperture with a diameter of 3 mm. The details of the VMI spectrometer and the conditions for the target D_2 molecule were described in [10]. An SiC concave mirror with a radius of curvature of 200 mm focuses the incident pulses.

The pulse duration of each field, except for the fundamental laser field, is expected to be less than 10 fs due to the fact that the measured spectra of the 3rd harmonic and 5th harmonic fields are both sufficiently broad to form a sub-10-fs pulse with small dispersions, as shown in Fig. 1(a). The peak intensity of the XUV (the 11th order harmonic) harmonic field is estimated to be of the order of 10^{13} W/cm^2, while those of the 5th harmonic, 3rd harmonic, and fundamental fields are all less than 10^{12} W/cm^2.

We show relevant potential energy curves against the nuclear distance of D_2 and D_2^+ in Fig. 1(b). The XUV high-order harmonic field of the 11th order with a photon energy of 17.1 eV and higher can ionize D_2 molecules by one-photon absorption and create a vibrational wave packet on the $1s\sigma_g$ potential curve of D_2^+. Nevertheless, we have concluded from nonlinear Fourier transform

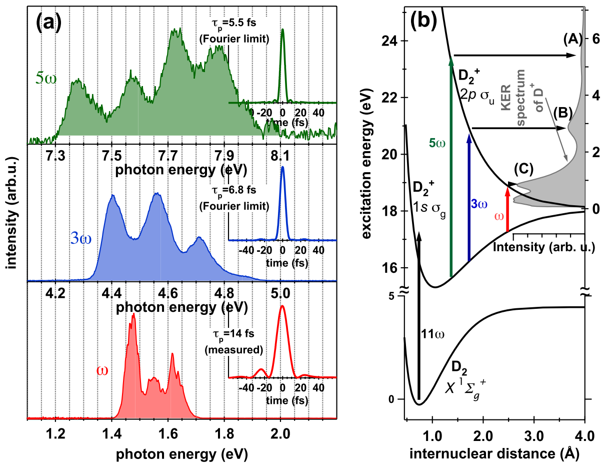

Fig. 1. (Color online) (a) Measured spectra of fundamental (ω), 3rd harmonic (3ω), and 5th harmonic (5ω) fields. The pulse shapes reconstructed with the measured phase (ω) and constant phase (3ω and 5ω) are shown in insets. (b) Relevant energy diagram of D_2 and D_2^+ and measured kinetic energy release (KER) spectrum.

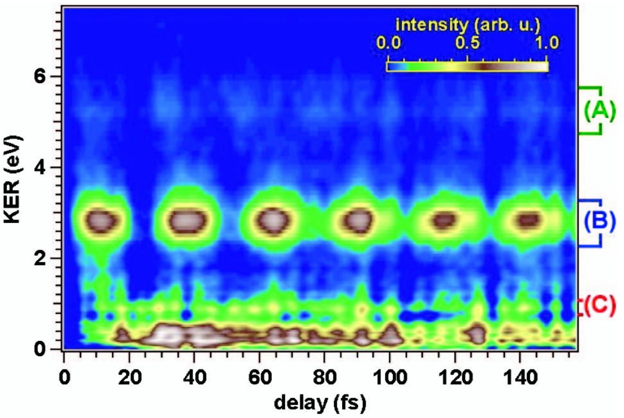

Fig. 2. Measured delay-KER spectrogram with constant background subtracted. The three KER components labeled (A), (B), and (C) are assigned to the fragmentation processes induced by absorbing the 5th, 3rd, and fundamental fields in the probe pulse, respectively.

spectroscopy (NFTS) [10] that the 11th-order harmonic field mainly contributes the formation of this wave packet. This is the reason why the advanced pulse acts as a pump with XUV photoabsorption. Then, the delayed pulse excites the D_2^+ in the $1s\sigma_g$ state to the $2p\sigma_u$ state by absorbing one photon of the 5th harmonic, 3rd harmonic, or fundamental field after some delay from the ionization. The transition amplitude tends to be large at the nuclear distance where the energy difference between the $1s\sigma_g$ and $2p\sigma_u$ potentials is close to the photon energy. Hence, we can find the PWP components in the whole generated wave packet by determining and analyzing the kinetic energy release (KER) spectrum from the observed D^+ fragments. We note that the harmonic fields higher than the 5th order may induce the one-photon transitions from the $1s\sigma_g$ to $2p\sigma_u$ states. We could not, however, observe the KER spectrum resulting from these transitions due to the low magnitude of the dipole at a small nuclear distance. This is the reason why the delayed pulse acts as a three-color probe.

The measured KER spectrum of D^+ at a fixed delay ($\tau \simeq 0$ fs) is shown as a hatched area in Fig. 1(b). The spectrum exhibits three distinct parts labeled (A) around 5.2 eV, (B) around 2.8 eV, and (C) around 0.8 eV. These three parts originate from the excitation with the three-color fields in the probe pulse. We have already shown how we assign the excitation process in [10].

We obtain a delay-KER spectrogram by scanning delay with a temporal step of 0.14 fs and a delay of approximately 150 fs, as shown in Fig. 2. We have processed the raw data to correct the unimportant linear decrease of the spectral intensity relative to delay, the interference fringes of the probe pulse near the delay origin, and the constant background signal to obtain this figure. We can notice the periodic modulation of the D^+ yield, in accordance with the delay in regions (A) and (B), respectively. This is clear evidence of the vibrational motion of D_2^+. We show area profiles in regions (A), (B), and (C) as solid curves in the top, middle, and bottom panels of Fig. 3(a), respectively. These traces are obtained by integrating the delay-KER spectrogram with respect to the KER around the peaks within a range of ±0.5, 0.5, and 0.17 eV for regions (A), (B), and (C), respectively. We can recognize periodic modulation in the solid curves in the top, middle, and bottom panels of Fig. 3(a), while the modulation period is different in each case. This feature of the modulation period is more evident in Fig. 3(b), which shows the absolute squares of the magnitudes of the Fourier transforms (FTs) of the solid curves in Fig. 3(a). The primary peak of the frequency spectrum in the top panel of Fig. 3(b) is located around 45 THz, and consequently the principal period of the modulation

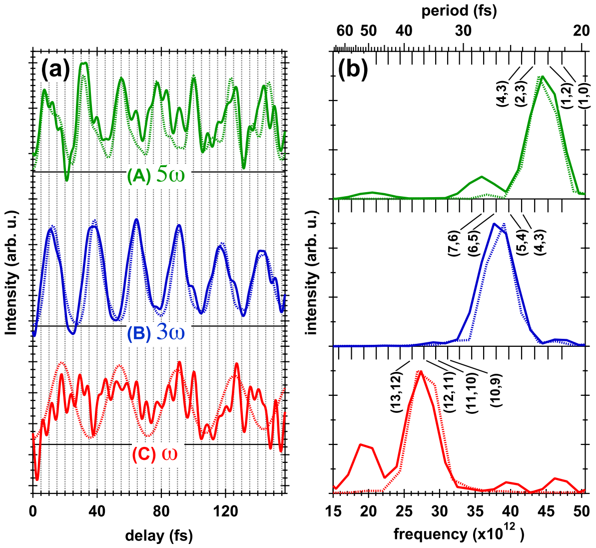

Fig. 3. (Color online) (a) Area profiles of the KER-delay spectrogram in region (A) (top panel), region (B) (middle panel), and region (C) (bottom panel), shown in Fig. 2; (b) the absolute squares of the magnitude of the Fourier transforms of the solid curves in the top, middle, and bottom panels of (a), plotted in the top, middle, and bottom panels, respectively. The long marks at the top axis of (b) indicate the energy differences between the pairs of adjacent vibrational levels shown in parentheses. The dotted curves in all the figures are the calculated results.

in Fig. 3(a) should be 22 fs. The monotonic decrease of the peak frequency following the decrease of the principal photon energy of the probe pulse field, shown in the top, middle, and bottom panels of Fig. 3(b), proves that the relevant vibrational levels in the wave packet are extracted and resolved with the three-color probe pulse. The additional subpeaks in these spectra are artifacts with the rectangular window in the FT calculation.

We have assigned the quantum number of the vibrational states extracted with each photon energy field in the probe pulse by comparing the frequency spectrum with the energy difference between adjacent vibrational states. The energy differences are depicted at the top axis in each panel of Fig. 3(b) as long marks. Note that the resolution of the frequency spectrum is restricted by the limitation of the scanning range of the delay, which is estimated to be ~ 7 THz $\simeq 1/(150$ fs$)$, and hence, we could not resolve the difference frequency corresponding to each long mark.

This experimental result for the probe process of the vibrational wave packet can be explained within a framework of the elementary time-dependent perturbation theory of interactions. By assuming the simple two-level system for the electronic state [14,15], we calculated the delay-KER spectrogram. The details of the model and calculation will be presented elsewhere. The calculated delay-KER spectrogram agrees well with the experimental data except in the KER region lower than 0.4 eV, although we do not show the figure. The similarity of the calculated result can be seen clearly in Figs. 3(a) and 3(b). The dotted curves in all these figures are obtained from the calculated spectrogram by data processing procedures similar to those adopted for the experimental data. In particular, the measured trace probed with the third harmonic field [solid curve in the middle panel of Fig. 3(a)] very closely coincides with the calculated result. The intensity profiles of the Fourier transforms of the calculated traces in the top, middle, and bottom panels of Fig. 3(b) also support the experimental results. Thus, we conclude our model calculation is feasible for simulating the probe process with a multicolor field.

In summary, we have demonstrated the experimental observation of time evolution of the vibrational motion of the D_2^+ molecule using the harmonic fields of a sub-15-fs Ti:sapphire laser pulse as an XUV pump and three-color probe pulses.

This work was carried out as part of the Advanced Photon Science Alliance (APSA) project commissioned by the Ministry of Education, Culture, Sports, Science, and Technology (MEXT). Y. Nabekawa gratefully acknowledges financial support by a grant for Scientific Research (A) from the Japan Society of the Promotion of Science (21244066). K. Midorikawa directed this research with a grant from MEXT for the Extreme Photonics Research Group in RIKEN.

References

1. M. Dantus, R. M. Bowman, and A. H. Zewail, Nature **343**, 737 (1990).
2. H. Katsuki, H. Chiba, B. Girard, C. Meier, and K. Ohmori, Science **311**, 1589 (2006).
3. C. R. Calvert, W. A. Bryan, W. R. Newell, and I. D. Williams, Phys. Rep. **491**, 1 (2010).
4. Y. H. Jiang, A. Rudenko, J. F. Pérez-Torres, O. Herrwerth, L. Foucar, M. Kurka, K. U. Kühnel, M. Toppin, E. Plésiat, F. Morales, F. Martín, M. Lezius, M. F. Kling, T. Jahnke, R. Dörner, J. L. Sanz-Vicario, J. van Tilborg, A. Belkacem, M. Schulz, K. Ueda, T. J. M. Zouros, S. Düsterer, R. Treusch, C. D. Schröter, R. Moshammer, and J. Ullrich, Phys. Rev. A **81**, 051402(R) (2010).
5. Y. Nabekawa, A. A. Eilanlou, Y. Furukawa, K. L. Ishikawa, H. Takahashi, and K. Midorikawa, Appl. Phys. B **101**, 523 (2010).
6. Y. Nabekawa, T. Shimizu, T. Okino, K. Furusawa, H. Hasegawa, K. Yamonouchi, and K. Midorikawa, Phys. Rev. Lett. **96**, 083901 (2006).
7. Y. Nabekawa, T. Shimizu, T. Okino, K. Furusawa, H. Hasegawa, K. Yamanouchi, and K. Midorikawa, Phys. Rev. Lett. **97**, 153904 (2006).
8. Y. Nabekawa, T. Shimizu, Y. Furukawa, E. J. Takahashi, and K. Midorikawa, Phys. Rev. Lett. **102**, 213904 (2009).
9. T. Okino, K. Yamanouchi, T. Shimizu, R. Ma, Y. Nabekawa, and K. Midorikawa, J. Chem. Phys. **129**, 161103 (2008).
10. Y. Furukawa, Y. Nabekawa, T. Okino, S. Saugout, K. Yamanouchi, and K. Midorikawa, Phys. Rev. A **82**, 013421 (2010).
11. T. K. Allison, T. W. Wright, A. M. Stooke, C. Khurmi, J. van Tilborg, Y. Liu, R. W. Falcone, and A. Belkacem, Opt. Lett. **35**, 3664 (2010).
12. I. Liontos, S. Cavalieri, C. Corsi, R. Eramo, S. Kaziannis, A. Pirri, E. Sali, and M. Bellini, Opt. Lett. **35**, 832 (2010).
13. L. H. Haber, B. Doughty, and S. R. Leone, Phys. Rev. A **79**, 031401(R) (2009).
14. U. Thumm, T. Niederhausen, and B. Feuerstein, Phys. Rev. A **77**, 063401 (2008).
15. F. He and U. Thumm, Phys. Rev. A **81**, 053413 (2010).